

# Stellar-Evolution Limits on Axion Properties

Georg Raffelt

Max-Planck-Institut für Physik, Föhringer Ring 6, 80805 München, Germany

If axions exist, they are copiously produced in hot and dense plasmas, carrying away energy directly from the interior of stars. Various astronomical observables constrain the operation of such anomalous stellar energy-loss channels and thus provide restrictive limits on the axion interactions with photons, nucleons, and electrons. In typical axion models a limit  $m_a \lesssim 10^{-2}$  eV is implied. The main arguments leading to this result are explained, including more recent work on the important supernova 1987A constraint.

## 1. INTRODUCTION

In the late 1950s, the existence of a direct neutrino-electron interaction was postulated in the context of the universal  $V-A$  theory of weak interactions. It was immediately recognized that it enables the production of neutrinos in stellar plasmas by thermal processes of the sort  $\gamma e^- \rightarrow e^- \bar{\nu} \nu$  or plasmon decay  $\gamma \rightarrow \bar{\nu} \nu$ . As neutrinos escape unscathed from normal stars, such processes effectively constitute a local energy sink for the nuclear reactions which power stars. Neutrino losses soon became a standard ingredient of stellar evolution theory [1] even though the details had to be modified when additional neutrino flavors and neutral-current interactions appeared.

New low-mass particles or nonstandard neutrino couplings would increase “invisible” stellar energy losses and thus modify the observed properties of stars, notably the duration of certain evolutionary phases. This “energy-loss argument” was first applied in 1963 to constrain neutrino dipole moments which would lead to nonstandard neutrino losses through an enhancement of the plasmon decay rate  $\gamma \rightarrow \bar{\nu} \nu$  [2]. A first application to “exotic” particles appeared in 1975 to constrain the coupling strength of putative light Higgs bosons [3]. Since then a large variety of cases has been studied, where axions were perhaps the greatest motivation for a systematic refinement of this method [4,5].

The purpose of this overview is to explain the stellar energy-loss argument in the context of the most important cases, to summarize the axion

limits obtained from this method, and to point at some open issues that require further research.

## 2. SUN

While the Sun does not provide the most restrictive astrophysical axion limits, it remains of interest as a source for previous [6], current [7] or proposed [8] experiments to search for the solar axion flux. Of particular interest is the axion-photon interaction

$$\mathcal{L}_{a\gamma} = g_{a\gamma} \mathbf{E} \cdot \mathbf{B} a, \quad (1)$$

where  $g_{a\gamma}$  is a coupling constant with the dimension  $(\text{energy})^{-1}$ ,  $\mathbf{E}$  and  $\mathbf{B}$  are the electric and magnetic fields, respectively, and  $a$  is the axion field. This interaction allows for the Primakoff conversion of photons into axions and vice versa (Fig. 1) and thus serves both as a production process in the Sun and as a detection process in “helioscope” experiments where one attempts to back-convert solar axions into detectable x-rays either in a dipole magnet or in a crystal [6–8]. The expected solar axion spectrum is shown in Fig. 2 for a coupling strength  $g_{a\gamma} = 10^{-10} \text{ GeV}^{-1}$ .



Figure 1. Primakoff production of axions.

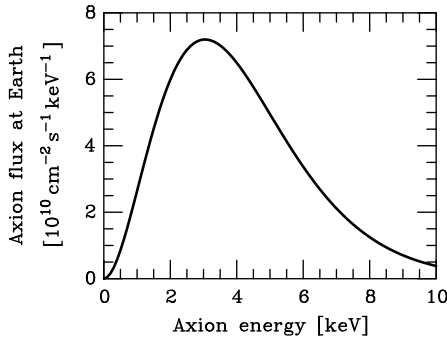


Figure 2. Solar axion flux at Earth from the Primakoff conversion of thermal photons in the Sun for  $g_{a\gamma} = 10^{-10} \text{ GeV}^{-1}$  [9].

The “standard Sun” is about halfway through its main-sequence evolution. Therefore, the solar axion luminosity must not exceed its photon luminosity or else its nuclear fuel would have been spent before reaching the current age of  $4.5 \times 10^9$  yr. This simple requirement yields [10]

$$g_{a\gamma} \lesssim 24 \times 10^{-10} \text{ GeV}^{-1}. \quad (2)$$

Interestingly, even such a large axion luminosity could be accommodated in a solar model by a suitable adjustment of the unknown presolar helium abundance.

The recent advance in helioseismology allows one to derive sound-speed profiles throughout the Sun—it is no longer enough for a solar model to reproduce the observed luminosity and radius at an age of  $4.5 \times 10^9$  yr. We are currently investigating if and how much one can improve on Eq. (2) by using helioseismological observations as a solar-model constraint [11].

### 3. GLOBULAR CLUSTERS

The most restrictive constraint on the axion-photon coupling as well as on a possible interaction with electrons arises from globular-cluster stars. Our galaxy has about 150 globular clusters such as M3 (Fig. 3), each consisting of a gravitationally bound system of typically  $10^6$  stars. The

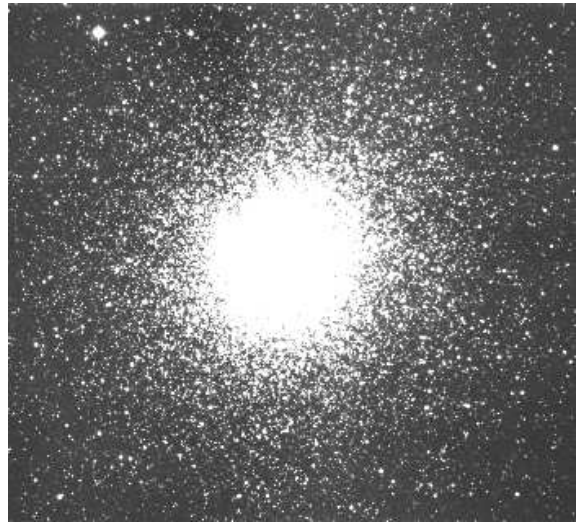


Figure 3. Globular cluster M3.

galactic globular-cluster system forms a roughly spherical halo—they are not located in the disk. The escape velocity from a typical cluster is only around  $10 \text{ km s}^{-1}$  so that a single supernova is enough to sweep it clean of all gas, preventing further star formation and thus guaranteeing almost equal stellar ages. In addition, all stars of a given cluster have nearly equal metallicities, where “metals” in astrophysical parlance are the elements heavier than helium. Therefore, the stars of a given cluster differ primarily in a single parameter, the initial mass, providing an ideal ensemble to test the theory of stellar evolution.

To this end one arranges the stars of a cluster in a color-magnitude diagram where one plots the color, representative of surface temperature, on the horizontal axis and the brightness on the vertical axis. One thus obtains a characteristic pattern (Fig. 4) where different branches correspond to different evolutionary phases which are schematically illustrated in Fig. 5.

The main sequence (MS) corresponds to central hydrogen burning and thus to normal stars like our own Sun. When the central hydrogen fuel is exhausted, the stars develop a degenerate he-

lium core, with hydrogen burning continuing in a shell. The luminosity is governed by the gravitational potential at the edge of the growing helium core—these stars become ever brighter as they ascend the red-giant branch (RGB). The higher a star is on the RGB the more massive (and compact) its helium core has become. Curiously, the envelope of these stars expands, leading to a large surface area and thus a low surface temperature (red color)—hence the name “red giant.”

The helium core grows until it reaches about  $0.5 M_{\odot}$  (solar mass) when it becomes dense and

hot enough to ignite helium. The ensuing core expansion reduces the gravitational potential at the edge and thus lowers the energy production rate in the hydrogen shell source. Helium ignition dims these stars, even though they now have two energy sources! The core masses are equal when helium ignites, but the envelope mass can differ due to varying rates of mass loss on the RGB, leading to different surface areas and thus surface temperatures. Therefore, after helium ignition the stars occupy the horizontal branch (HB) in the color-magnitude diagram.

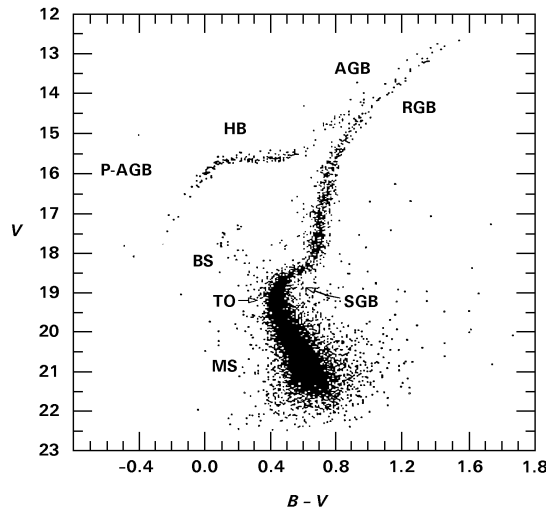


Figure 4. Color magnitude diagram for the globular cluster M3 [12], based on the photometric data of 10,637 stars. The classification for the evolutionary phases is as follows [13]. MS (main sequence): core hydrogen burning. BS (blue stragglers): central hydrogen is exhausted. SGB (subgiant branch): hydrogen burning in a thick shell. RGB (red-giant branch): hydrogen burning in a thin shell with a growing core until helium ignites. HB (horizontal branch): helium burning in the core and hydrogen burning in a shell. AGB (asymptotic giant branch): helium and hydrogen shell burning. P-AGB (post-asymptotic giant branch): final evolution from the AGB to the white-dwarf stage.

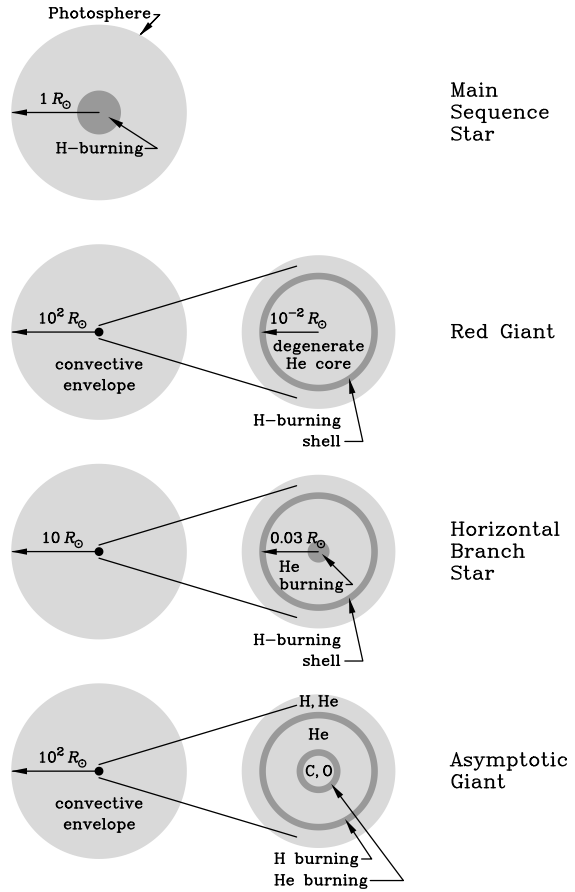


Figure 5. Evolutionary phases of low-mass stars. The envelope and core dimensions depend on the location on the RGB, HB, or AGB, respectively; the radii are given for a rough orientation.

Finally, when helium is exhausted, a degenerate carbon-oxygen core develops, leading to a second ascent on what is called the asymptotic giant branch (AGB). These low-mass stars cannot ignite their CO core. They become white dwarfs after shedding most of their envelope.

The advanced evolutionary phases are fast compared with the MS evolution of about  $10^{10}$  yr for stars with a total mass somewhat below  $1 M_{\odot}$ . For example, the ascent on the upper RGB and the helium-burning phase each take around  $10^8$  yr. Therefore, the distribution of stars along the RGB and beyond can be taken as an “isochrone” for the evolution of a single star, i.e. a time-series of snapshots for the evolution of a single star with a fixed initial mass. Put another way, the number distribution of stars along the different branches are a direct measure for the duration of the advanced evolutionary phases. The distribution along the MS is different in that it measures the distribution of initial masses.

The core temperature before and after helium ignition is about  $10^8$  K, but the average core density changes from  $2 \times 10^5$  g cm $^{-3}$  (degenerate) to  $0.6 \times 10^4$  g cm $^{-3}$  on the HB (nondegenerate). This implies that the Primakoff production of axions will be much more effective in the cores of HB stars than in those of upper RGB stars. The axionic energy loss on the HB would shorten the helium-burning phase because the nuclear fuel would be consumed faster, causing a reduction of the number of HB relative to RGB stars.

The number ratio of HB/RGB stars in 15 galactic globular clusters was measured in 1983 [14], yielding the results shown in Fig. 6 as a function of the logarithmic metallicity measure  $[\text{Fe}/\text{H}]$ . These data reveal that the duration of the helium-burning phase agrees within about 10% with the predictions of the standard stellar evolution theory, leading to the bound [5]

$$g_{a\gamma} \lesssim 0.6 \times 10^{-10} \text{ GeV}^{-1}. \quad (3)$$

This limit is slightly more restrictive than the often-quoted “red-giant bound” which was based on the same argument applied to open rather than globular clusters [10]. Open clusters are galactic-disk counterparts to globular clusters; they are less populous, leading to sparse num-

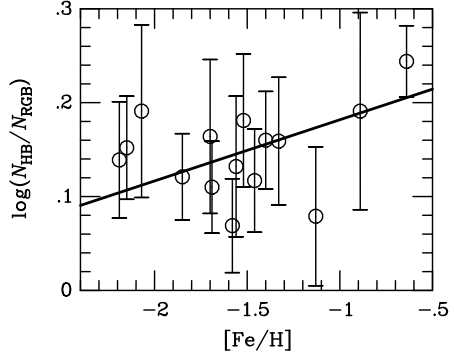


Figure 6. Number ratio of HB/RGB stars for 15 galactic globular clusters as a function of metallicity [14]. The thick line is a linear fit.

ber counts and hence to statistically less significant axion limits. Open clusters tend to have higher metallicities. As a result, the hydrogen-burning stars are not spread out along a horizontal branch, but occupy a common location, the “red-giant clump” at the base of the RGB. Hence the notion of the “red-giant bound” even though the argument as presented here is more appropriately called “globular-cluster bound.”

In terms of the Peccei-Quinn scale  $f_a$  or axion mass  $m_a$ , the axion-photon coupling is

$$g_{a\gamma} = -\frac{3\alpha}{8\pi f_a} \xi = -\frac{m_a/\text{eV}}{0.69 \times 10^{10} \text{ GeV}} \xi, \quad (4)$$

where

$$\xi \equiv \frac{4}{3} \left( \frac{E}{N} - 1.92 \pm 0.08 \right). \quad (5)$$

Here,  $E/N$  is a model-dependent ratio of small integers. In the DFSZ model or GUT models one has  $E/N = 8/3$ , corresponding to  $\xi \approx 1$ . In this case the globular cluster limit implies

$$m_a \lesssim 0.4 \text{ eV}. \quad (6)$$

However, one can construct models where  $E/N = 2$ , allowing for a near or complete cancellation of the axion-photon coupling. Naturally, in this case there is no globular-cluster limit on  $m_a$  or  $f_a$ .

One can use other observables in the color-magnitude diagram to test the theory of stellar evolution, such as the brightness difference between the HB and the tip of the RGB, the absolute brightness of the HB, and others.

In this way one can also derive limits on a putative axion-electron interaction. It is of the form

$$\mathcal{L}_{ae} = \frac{C_e}{2f_a} \bar{\psi}_e \gamma^\mu \gamma_5 \psi_e \partial_\mu a \quad (7)$$

which is usually equivalent to the pseudoscalar interaction  $-i(C_e m_e/f_a) \bar{\psi}_e \gamma_5 \psi_e a$ . One finds a limit to the Yukawa coupling of [15]

$$g_{ae} = C_e m_e / f_a \lesssim 2.5 \times 10^{-13}, \quad (8)$$

or  $\alpha_{26} \lesssim 0.5$  where  $\alpha_{26} = 10^{26} g_{ae}^2 / 4\pi$ . However, the existence of such a coupling is not generic to all axion models.

#### 4. WHITE DWARFS

If axions do interact with electrons, they are emitted from white dwarfs predominantly by the bremsstrahlung process  $e^- + Ze \rightarrow Ze + e^- + a$  and would thus accelerate the cooling of these degenerate stellar remnants. The observed white-dwarf luminosity function yields a limit on  $g_{ae}$  which is slightly weaker than Eq. (8).

Intriguingly, axion emission with  $\alpha_{26} \approx 0.45$ , just below the globular-cluster limit, might dominate the cooling of white dwarfs such as the ZZ Ceti star G117-B15A for which the cooling speed has been established by a direct measurement of the decrease of its pulsation period [16].

The most popular example where axions couple to electrons is the DFSZ model where  $C_e = \frac{1}{3} \cos^2 \beta$  with  $\beta$  an arbitrary angle. In this case one may use the SN 1987A limits on the axion-nucleon coupling (see below) to derive an indirect  $\beta$ -dependent limit on  $g_{ae}$ . From Ref. [18] I infer that the largest axion-electron coupling allowed by SN 1987A corresponds to  $\alpha_{26} \approx 0.08$ , suggesting that DFSZ axions are not responsible for the anomalous cooling speed of G117-B15A.

In magnetic white dwarfs, axion emission can be accelerated by the cyclotron process [17]. However, it appears that one needs unreasonably strong  $B$  fields to obtain a significant effect.

#### 5. SUPERNOVA 1987A

Being a QCD phenomenon, axions generically couple to nucleons. The most significant limit on this coupling arises from the cooling speed of nascent neutron stars as established by the duration of the neutrino signal from the supernova (SN) 1987A. It also implies the most restrictive constraints on  $f_a$  and  $m_a$ .

A type II supernova explosion is physically the implosion of the degenerate iron core of a massive star which has gone through all possible burning phases. As iron is the most tightly bound nucleus, further energy gain by nuclear fusion is not possible so that the core becomes unstable when it has reached the limiting mass (Chandrasekhar mass) that can be supported by electron degeneracy pressure. The ensuing collapse is intercepted when the equation of state (EOS) stiffens at nuclear density, i.e. the core mass of  $1\text{--}2 M_\odot$  collapses to the size of a few ten kilometers across. At nuclear densities ( $\rho_0 = 3 \times 10^{14} \text{ g cm}^{-3}$ ) and temperatures of tens of MeV, this compact object is opaque to neutrinos which are thus trapped. Therefore, the gravitational binding energy of the newly formed neutron star (“proto neutron star”) of about  $3 \times 10^{53}$  ergs is radiated over several seconds from the “neutrino sphere.” Crudely put, the collapsed SN core cools by blackbody neutrino emission from its surface.

The neutrinos from a collapsed star were observed once, on 23 Feb. 1987, when the blue supergiant Sanduleak -69 202 in the Large Magellanic Cloud (a small satellite galaxy of our Milky Way at a distance of about 165,000 light years) exploded—the legendary SN 1987A. The neutrinos were registered by the Kamiokande [19] and IMB [20] water Cherenkov detectors and the Baksan Scintillator Telescope (BST) [21]—see Fig. 7 for a summary of the data. The number of events, their energies, and the distribution over several seconds corresponds well to what is theoretically expected and has thus been taken as a confirmation of the picture that in a type II supernova a compact remnant forms which emits its energy by quasi-thermal neutrino emission.

In analogy to the energy-loss argument for normal stars, the emission of axions would com-

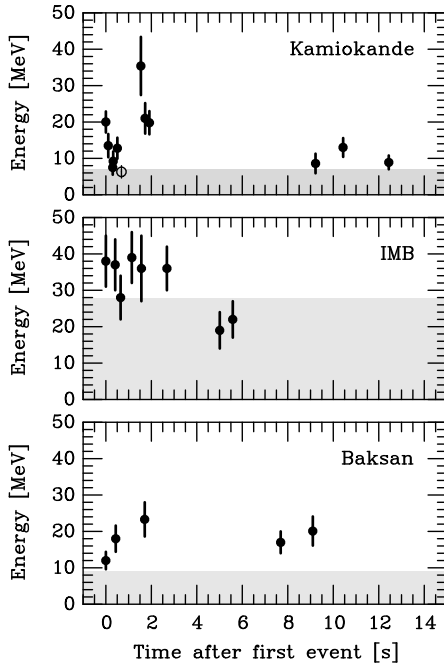


Figure 7. SN 1987A neutrino observations at Kamiokande [19], IMB [20] and Baksan [21]. The energies refer to the secondary positrons from the reaction  $\bar{\nu}_e p \rightarrow n e^+$ , not the primary neutrinos. In the shaded area the trigger efficiency is less than 30%. The clocks have unknown relative offsets; in each case the first event was shifted to  $t = 0$ . In Kamiokande, the event marked as an open circle is attributed to background.

pete with the standard cooling channel, in the present case neutrinos, and would thus remove energy from the neutrino signal. Axions would be produced by nucleon-nucleon bremsstrahlung (Fig. 8) in the inner SN core and would escape directly from there. Therefore, they would primarily remove the energy which powers the late-time neutrino emission so that their main effect would be to shorten the expected neutrino signal, in contrast with the observations [22,23].

Of course, if the axion coupling were too strong, then they would be trapped like neutrinos and emerge as thermal radiation from an appropriate

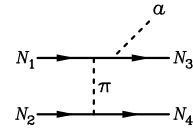


Figure 8. Nucleon-nucleon bremsstrahlung emission of axions.

“axiosphere” near the surface of the proto neutron star [23]. Therefore, the existence of axions is compatible with the SN 1987A neutrino signal if axions are either very weakly or relatively strongly interacting.

This general insight was backed up by detailed numerical simulations, some of which are summarized in Fig. 9. The total energy emitted in axions and neutrinos, the total number of neutrino events expected in the Kamiokande and IMB detectors, and the signal duration are each shown as a function of the assumed axion-nucleon Yukawa coupling which was taken to be the same for protons and neutrons. The interaction has the general derivative structure

$$\mathcal{L}_{aN} = \frac{C_N}{2f_a} \bar{\psi}_N \gamma^\mu \gamma_5 \psi_N \partial_\mu a. \quad (9)$$

The Yukawa coupling is  $g_{aN} \equiv C_N m_N / f_a$  in analogy to the electron coupling. In general the dimensionless numerical coefficients  $C_N$  will be different for protons and neutrons. From Fig. 9 it is evident that for a certain window of coupling constants the neutrino signal would be significantly shortened.

It must be stressed that axions on the “strong interaction” side of this window are not necessarily allowed because they themselves could be registered in the water Cherenkov detectors as they could be absorbed by nuclei which can then de-excite by  $\gamma$  emission [25].

A significant problem with the supernova argument is the difficulty of calculating the axion emission rate in a hot and dense nuclear medium. The early bremsstrahlung calculations were based on a “naive” evaluation of the perturbative amplitude of Fig. 8. However, when one

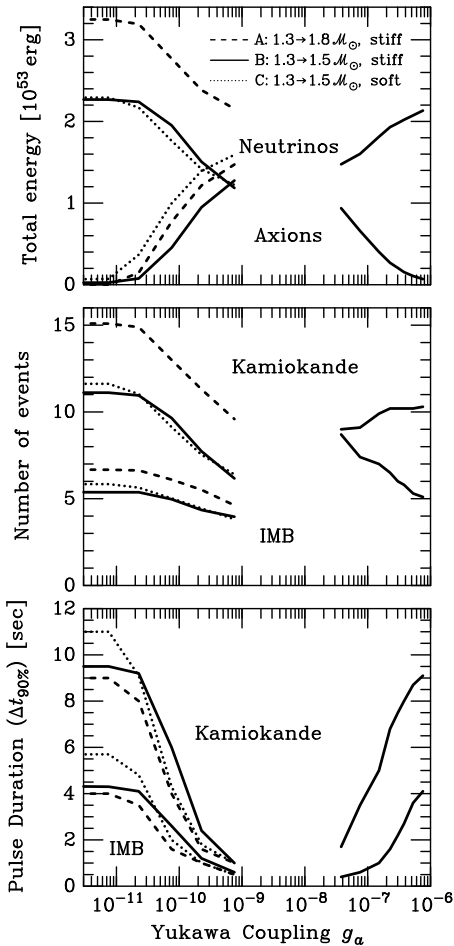


Figure 9. Results from numerical protoneutron star cooling sequences with axions. The free-streaming regime (small  $g_a$ ) is taken from Ref. [26], the trapping regime (large  $g_a$ ) from Ref. [27]. For models A, B, and C (corresponding to models 57, 55, and 62 of Ref. [28]) the amount of early accretion and the equation of state (“stiff” or “soft”) is indicated. The models were calculated until 20 s after collapse.

looks at this problem from the more general perspective of linear-response theory one can easily show that such a calculation is not self-consistent. The derivative coupling of Eq. (9) implies that

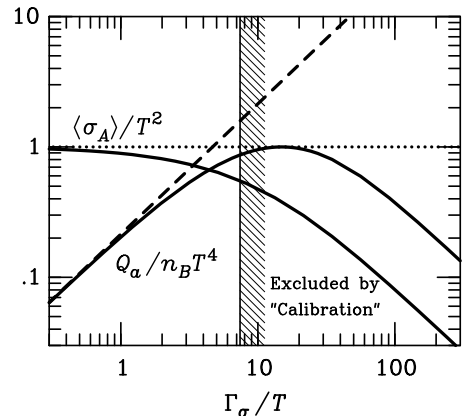


Figure 10. Axion emission rate and thermally averaged neutrino scattering cross section as a function of the assumed spin fluctuation rate in a nuclear medium [24]. The dotted and dashed lines represent the “naive” perturbative behavior. The duration of the SN 1987A neutrino signal excludes  $\Gamma_\sigma$  to the right of the hatched band.

in the nonrelativistic limit axions couple to the nucleon spins. Therefore, what emits the axions are the nucleon spins which themselves are being kicked around by spin-dependent forces among each other. Therefore, the spin-fluctuation rate  $\Gamma_\sigma$ , roughly the rate at which a nucleon spin is flipped in collisions, is an intuitive measure of the microscopic event rate that leads to the emission of axions. On rather general grounds one can show that the axion emission rate per nucleon as a function of  $\Gamma_\sigma$  first increases, but later it turns over and actually decreases as indicated in Fig. 10, a behavior which is naturally understood in terms of multiple scatterings in the spirit of the Landau-Pomeranchuk-Migdal effect [24].

A perturbative calculation of  $\Gamma_\sigma$ , based on a one-pion exchange potential, reveals that  $\Gamma_\sigma/T$  is 30–50 for the conditions of a SN core. Such large values likely are significant overestimates. An empirical reason for this conclusion is based on the SN 1987A signal duration. To this end observe that neutrinos couple to nucleons by an axial-vector interaction. Their vector-current contri-

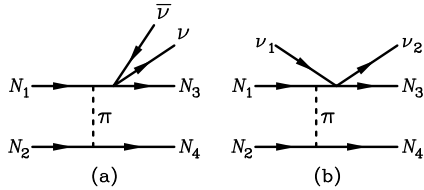


Figure 11. Nucleon bremsstrahlung emission of neutrino pairs and the corresponding “inelastic scattering” amplitude.

bution to scattering cross sections is smaller than the axial-current contribution by a factor of a few so that we may ignore it at a first crude level of approximation. Then it is clear that neutrino pairs can be emitted in bremsstrahlung processes in full analogy to axions, but also that spin fluctuations will affect the neutrino elastic scattering cross section (Fig. 11). One can again show on the basis of general linear-response theory arguments that this effect leads to a reduction of the axial-current scattering cross section. Graphically this may be pictured as a reduction of the nucleon “average spin” seen by neutrinos due to spin-flipping nucleon-nucleon interactions. The expected average cross-section reduction as a function of  $\Gamma_\sigma$  is shown in Fig. 10. A large neutrino cross-section reduction would make the proto neutron star more transparent to neutrinos and thus would allow them to escape more quickly, unduly shortening the SN 1987A signal. This argument suggests that values of  $\Gamma_\sigma$  to right of the hatched band in Fig. 10 are excluded.

A quantitative understanding of both axion emissivities and neutrino opacities in a hot and dense nuclear medium requires a reliable calculation of the dynamical spin and isospin structure functions, a task which is currently out of reach. It is possible, and even expected, that nucleon correlations beyond the above simple multiple-scattering effects provide significant modifications of the neutrino opacities [29] and thus also of the axion emissivities.

Unless there is some huge unexpected cancellation, however, the axion emissivities likely

are near the maximum indicated in Fig. 10. Based on this assumption, limits on the axion-nucleon coupling have been both estimated [24] and calculated from detailed numerical cooling sequences [18] which are not very different from the ones shown in Fig. 9 except that the axion emission rate is suppressed according to the schematic picture of Fig 10.

In order to translate the limits on the axion-nucleon couplings into limits on the Peccei-Quinn scale or axion mass one must use specific models. For KSVZ axions, where the axion-neutron coupling nearly vanishes, the SN 1987A limit is  $m_A \lesssim 0.008$  eV, while it varies between about 0.004 and 0.012 eV for DFSZ axions, depending on the angle  $\beta$  which measures the ratio of two Higgs vacuum expectation values [18]. In view of the large overall uncertainties it is good enough to remember  $m_A \lesssim 0.01$  eV as a generic limit.

## 6. COSMOLOGY

While axion cosmology is not the topic of this overview (various aspects are covered by other speakers at this conference), a few remarks are in order to explain my summary plot Fig. 12.

In the early universe, axions come into thermal equilibrium if  $f_a \lesssim 10^8$  GeV [30], a region excluded by the stellar-evolution limits. If inflation occurred after the Peccei-Quinn symmetry breaking or if  $T_{\text{reheat}} < f_a$ , the “misalignment mechanism” [31] leads to a contribution to the cosmic critical density of  $\Omega_a h^2 \approx 1.9 \times 3^{\pm 1} (1 \mu\text{eV}/m_a)^{1.175} \Theta_i^2 F(\Theta_i)$  where  $h$  is the Hubble constant in units of  $100 \text{ km s}^{-1} \text{ Mpc}^{-1}$ . The stated range reflects uncertainties of the cosmic conditions at the QCD phase transition and of the temperature-dependent axion mass. The function  $F(\Theta)$  with  $F(0) = 1$  and  $F(\pi) = \infty$  accounts for anharmonic corrections to the axion potential. Because the initial misalignment angle  $\Theta_i$  can be very small or very close to  $\pi$ , there is no real prediction for the mass of dark-matter axions even though one would expect  $\Theta_i^2 F(\Theta_i) \sim 1$  to avoid fine-tuning the initial conditions.

A possible fine-tuning of  $\Theta_i$  is limited by inflation-induced quantum fluctuations which in turn lead to temperature fluctuations of the cos-

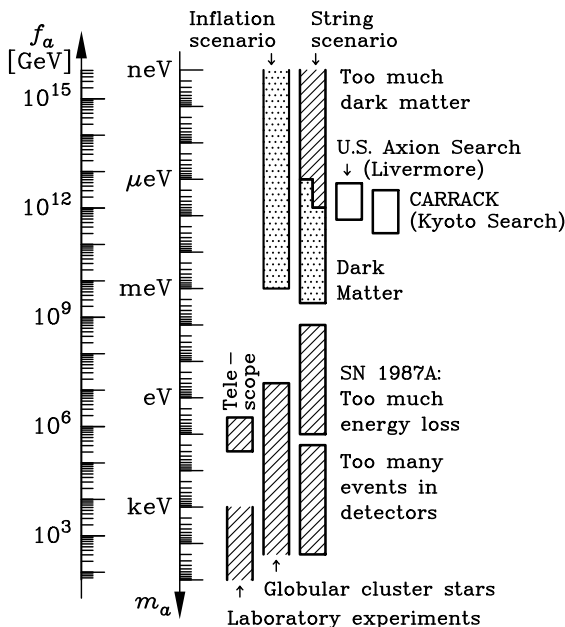


Figure 12. Astrophysical and cosmological exclusion regions (hatched) for the axion mass  $m_a$  or equivalently, the Peccei-Quinn scale  $f_a$ . An “open end” of an exclusion bar means that it represents a rough estimate; its exact location has not been established or it depends on detailed model assumptions. The globular cluster limit depends on the axion-photon coupling; it was assumed that  $E/N = 8/3$  as in GUT models or the DFSZ model. The SN 1987A limits depend on the axion-nucleon couplings; the shown case corresponds to the KSVZ model and approximately to the DFSZ model. The dotted “inclusion regions” indicate where axions could plausibly be the cosmic dark matter. Most of the allowed range in the inflation scenario requires fine-tuned initial conditions. In the string scenario the plausible dark-matter range is controversial as indicated by the step in the low-mass end of the “inclusion bar.” Also shown is the projected sensitivity range for the galactic dark-matter search experiments.

mic microwave background [32,33]. In a broad class of inflationary models one thus finds an upper limit to  $m_a$  where axions could be the dark matter. According to the most recent discussion [33] it is about  $10^{-3}$  eV (Fig. 12).

If inflation did not occur at all or if it occurred before the Peccei-Quinn symmetry breaking with  $T_{\text{reheat}} > f_a$ , cosmic axion strings form by the Kibble mechanism [34]. Their motion is damped primarily by axion emission rather than gravitational waves. After axions acquire a mass at the QCD phase transition they quickly become nonrelativistic and thus form a cold dark matter component. The axion density such produced is similar to that from the misalignment mechanism for  $\Theta_i = \mathcal{O}(1)$ , but in detail the calculations are difficult and somewhat controversial between two groups of authors [35,36]. Taking into account the uncertainty in various cosmological parameters one arrives at a plausible range for dark-matter axions as indicated in Fig. 12.

If axions are indeed the dark matter of our galaxy one can search for them with the “haloscope method.” At the present time two full-scale “second generation” axion haloscopes are in operation, one in Livermore (California) [37] and one in Kyoto (Japan) [38], the latter one using a beam of Rydberg atoms as a low-noise microwave detector. The projected sensitivity range shown in Fig. 12 covers the lower end of the plausible mass range for dark-matter axions.

## 7. SUMMARY

By virtue of their close relationship to neutral pions, axions couple generically to photons and nucleons, allowing for the production of axions in the hot and dense interior of various types of stars. Number counts of globular-cluster stars reveal that the duration of the advanced evolutionary phases of these low-mass stars agrees well with standard predictions, excluding the operation of a strong anomalous energy-loss channel. The SN 1987A neutrino signal further indicates that axions with a mass exceeding about  $10^{-2}$  eV would unduly shorten the cooling time of a proto neutron star. Taken together, these limits suggest that axions, if they exist, play a cosmologi-

cal dark-matter role, at least in the framework of a scenario where primordial axions are produced by string radiation rather than the misalignment mechanism.

One interesting loop-hole arises in axion models where the coupling to photons is very small because  $E/N = 2$  in Eq. (5), leading to a cancellation effect. In this case there is a narrow window of allowed axion masses around a few eV on the strong-interaction side of the SN 1987A limit. Intriguingly, axions in this window would be important as a hot dark matter component [39].

From the perspective of stellar-evolution tests of the axion hypothesis, it remains to be hoped that we will be lucky and see a galactic supernova with a large detector such as Superkamiokande to obtain a high-statistics neutrino signal. Meanwhile, more work is needed on the microscopic input physics for numerical supernova studies, both for the sake of a better understanding of the supernova phenomenon and its application as a laboratory for fundamental physics.

## ACKNOWLEDGMENTS

Partial support by the Deutsche Forschungsgemeinschaft under grant No. SFB-375 is acknowledged.

## REFERENCES

1. D.D. Clayton, *Principles of Stellar Evolution and Nucleosynthesis* (University of Chicago Press, 1968). R. Kippenhahn and A. Weigert, *Stellar Structure and Evolution* (Springer, Berlin, 1990).
2. J. Bernstein, M.A. Ruderman and G. Feinberg, Phys. Rev. **132**, 1227 (1963).
3. K. Sato and H. Sato, Prog. Theor. Phys. **54**, 1564 (1975).
4. M.S. Turner, Phys. Rept. **197**, 67 (1990). G.G. Raffelt, Phys. Rept. **198**, 1 (1990).
5. G. Raffelt, *Stars as Laboratories for Fundamental Physics* (University of Chicago Press, Chicago, 1996).
6. D.M. Lazarus et al., Phys. Rev. Lett. **69**, 2333 (1992).
7. P.V. Vorob'ev, A.I. Kakhidze and I.V. Kolokolov, Yad. Fiz. **58**, 1032 (1995) [Phys. At. Nucl. **58**, 959 (1995)]. F.T. Avignone III et al. (SOLAX Collaboration), astro-ph/9708008, submitted to Phys. Lett. B, and these proceedings. M. Minowa, these proceedings.
8. K. Zioutas et al., astro-ph/9801176, submitted to Nucl. Instrum. Meth. A.
9. K. van Bibber, D. Morris, P. McIntyre, and G. Raffelt, Phys. Rev. D **39**, 2089 (1989).
10. G. Raffelt and D. Dearborn Phys. Rev. D **36**, 2211 (1987).
11. H. Schlattl, A. Weiss and G. Raffelt, *Helioseismological constraints on solar axion emission*, work in progress (1998).
12. R. Buonanno et al., Mem. Soc. Astron. Ital. **57**, 391 (1986).
13. A. Renzini and F. Fusi Pecci, Ann. Rev. Astron. Astrophys. **26**, 199 (1988).
14. A. Buzzoni et al., Astron. Astrophys. **128**, 94 (1983).
15. G.G. Raffelt and A. Weiss, Phys. Rev. D **51**, 1495 (1995).
16. J. Isern, M. Hernanz and E. Garcia-Berro, Astrophys. J. **392**, L23 (1992).
17. M. Kachelriess, C. Wilke and G. Wunner, Phys. Rev. D **56**, 1313 (1997).
18. W. Keil et al., Phys. Rev. D **56**, 2419 (1997).
19. K.S. Hirata et al., Phys. Rev. D **38**, 448 (1988).
20. C.B. Bratton et al., Phys. Rev. D **37**, 3361 (1988).
21. E.N. Alexeyev et al., Pis'ma Zh. Eksp. Teor. Fiz. **45**, 461 (1987) [JETP Lett. **45**, 589 (1987)].
22. J. Ellis and K.A. Olive, Phys. Lett. B **193**, 525 (1987). G. Raffelt and D. Seckel, Phys. Rev. Lett. **60**, 1793 (1988).
23. M. Turner, Phys. Rev. Lett. **60**, 1797 (1988).
24. H.-T. Janka, W. Keil, G. Raffelt and D. Seckel, Phys. Rev. Lett. **76**, 2621 (1996).
25. J. Engel, D. Seckel and A.C. Hayes, Phys. Rev. Lett. **65**, 960 (1990).
26. A. Burrows, M.S. Turner and R.P. Brinkmann, Phys. Rev. D **39**, 1020 (1989).
27. A. Burrows, T. Ressell and M.S. Turner, Phys. Rev. D **42**, 3297 (1990).
28. A. Burrows, Astrophys. J. **334**, 891 (1988).

- 29. A. Burrows and R. Sawyer, to be published in Phys. Rev. C, astro-ph/9801082.
- 30. M. Turner, Phys. Rev. Lett. **59**, 2489 (1987).
- 31. J. Preskill, M. Wise and F. Wilczek, Phys. Lett. B **120**, 127 (1983). L. Abbott and P. Sikivie, *ibid.* 133. M. Dine and W. Fischler, *ibid.* 137. M.S. Turner, Phys. Rev. D **33**, 889 (1986).
- 32. D.H. Lyth, Phys. Lett. B **236**, 408 (1990). M.S. Turner and F. Wilczek, Phys. Rev. Lett. **66**, 5 (1991). A. Linde, Phys. Lett. B **259**, 38 (1991).
- 33. E.P.S. Shellard and R.A. Battye, “Inflationary axion cosmology revisited”, in preparation (1998); the main results can be found in: E.P.S. Shellard and R.A. Battye, astro-ph/9802216.
- 34. R.L. Davis, Phys. Lett. B **180**, 225 (1986). R.L. Davis and E.P.S. Shellard, Nucl. Phys. B **324**, 167 (1989).
- 35. R.A. Battye and E.P.S. Shellard, Nucl. Phys. B **423**, 260 (1994); Phys. Rev. Lett. **73**, 2954 (1994); (E) *ibid.* **76**, 2203 (1996); astro-ph/9706014, to be published in: Proc. Dark Matter 96, Heidelberg, ed. by H.V. Klapdor-Kleingrothaus and Y. Ramacher.
- 36. D. Harari and P. Sikivie, Phys. Lett. B **195**, 361 (1987). C. Hagmann and P. Sikivie, Nucl. Phys. B **363**, 247 (1991).
- 37. C. Hagmann et al., Phys. Rev. Lett. **80**, 2043 (1998).
- 38. I. Ogawa, S. Matsuki and K. Yamamoto, Phys. Rev. D **53**, R1740 (1996).
- 39. T. Moroi and H. Murayama, hep-ph/9804291.